European Journal of Ophthalmology / Vol. 18 no. 2, 2008 / pp. 239-247

Correlation of visual function impairment and OCT findings in patients with Stargardt disease and fundus flavimaculatus

G. QUERQUES[1,3], R. PRATO[2], C. IACULLI[3], M. VOIGT[1], N. DELLE NOCI[3], G. COSCAS[1], G. SOUBRANE[1], E.H. SOUIED[1]

[1]Department of Ophthalmology, Hopital Intercommunal de Creteil, University Paris XI, Paris - France
[2]Department of Hygiene
[3]Department of Ophthalmology, Ospedali Riuniti, University of Foggia, Foggia - Italy

PURPOSE. *To investigate the relationship between morphologic lesions of the retina and functional abnormalities in patients with Stargardt disease (STGD) and fundus flavimaculatus (FFM).*
DESIGN. *Case-controlled, prospective, comparative observational study.*
METHODS. *A complete ophthalmologic examination, including best-corrected visual acuity (BCVA) and optical coherence tomography (OCT), was performed in 61 eyes of 32 consecutive patients with STGD/FFM and in 60 eyes of 30 matched healthy control subjects. Furthermore, fundus-related perimetry was performed in 12 of the affected eyes.*
RESULTS. *The age ranged from 21 to 71 years in STGD/FFM patients and from 21 to 72 years in controls. BCVA ranged from 20/20 to 20/400 and from 20/20 to 20/32, respectively, in STGD/FFM patients and in controls. A foveal thinning was found by OCT Stratus in almost all cases (average 160 μm) compared with controls (average 210 μm) ($p<0.001$). BCVA impairment significantly correlated to the degree of foveal thinning ($r2=0.16$; $p=0.0014$). Moreover, in STGD/FFM patients the authors observed two types of hyperreflective deposits which were not correlated with BCVA impairment or foveal thinning. In addition, fundus-related perimetry revealed a stable fixation in 8/12 eyes, that was predominantly central in only 4 of these eyes. A smaller degree of foveal thinning correlated to a more stable fixation ($p=0.0108$), even if not predominantly central ($p=0.0218$).*
CONCLUSIONS. *In this series, lower visual acuity and unstable fixation correlated with a greater transverse foveal thinning. OCT and fundus-related perimetry may be useful tools in STGD/FFM patients. (Eur J Ophthalmol 2008; 18: 239-47)*

KEY WORDS. *Fundus flavimaculatus, Fundus-related perimetry, Microperimetry, Optical coherence tomography, Retinal dystrophy, Stargardt disease*

Accepted: October 2, 2007

INTRODUCTION

Stargardt disease (STGD), described by Karl Stargardt in 1909 (1-3), and fundus flavimaculatus (FFM), a Stargardt-like phenotype described by Franceschetti in 1965 (4), are variants of the same hereditary disease that affects the retinal pigment epithelium (RPE) and photoreceptor layer, both linked with the *ABCA4* gene (5-7). The disease is usually termed STGD when characterized by a juvenile onset (first 2 decades), a rapidly progressive course, and a poor visual outcome; the term FFM is favored when the disease begins at the end of the second decade or within the third decade and has a slowly progressive course (8, 9). The general course of STGD and FFM is a progressive loss of central vision (≤20/200), resulting in central atrophy and thus loss of central visual function. The yellowish-white well-defined perifoveal deposits called "flecks" are usual features of the early stage of both Stargardt disease

 1120-6721/239-09$25.00/0

and FFM. At this stage, the reduction of visual acuity is not concomitant with the severity of the fundus lesion (10-12). At the end stage, there is a large retinal central atrophy extended into the deeper layers of the posterior pole, and thus it is difficult to distinguish the flecks on fundus examination, although clearly revealed by fundus autofluorescence (AF) (13-15) and optical coherence tomography (OCT) (16). The pace of visual loss remains unpredictable (17, 18). Therefore, a qualitative and quantitative method that correlates the retinal status with functional impairment would be useful in determining the disease prognosis.

In this study, we investigated the relationship between the clinical data from some OCT parameters, such as foveolar thickness (FT) and type of flecks, and some functional values, such as best-corrected visual acuity (BCVA) and fixation location and stability.

METHODS

Sixty-one eyes from 32 consecutive patients with STGD and FFM macular dystrophy were prospectively included in this study. Informed consent was obtained according to both a Foggia University and a Paris XII University Institutional Review Board–approved protocol. Criteria for inclusion were age >18 years, presence of retinal flecks on fundus examination, evidence of autofluorescence of the retinal flecks, and diagnosis of dark choroid on fluorescein angiography (FA). Eyes presenting with any associated macular diseases or complication, such as, respectively, myopia >–8 D, angioid streaks, confluent drusen, and epiretinal membrane, or choroidal neovascularization, were excluded from this study. All patients, as well as 30 age-similar healthy control subjects (60 eyes), underwent a complete ophthalmologic examination, including assessment of best-corrected visual acuity (BCVA), fundus biomicroscopy, color photography of the fundus (Canon 60 fundus camera, Tokyo, Japan; Topcon TRC-50 retinal camera, Tokyo, Japan; Zeiss FF 450 plus, Carl Zeiss AG, Germany), autofluorescence frames (confocal on Heidelberg Retina Angiograph Heidelberg Engineering, Heidelberg, Germany, or non confocal on Canon 60 fundus camera; Topcon TRC-50 retinal camera; Zeiss FF 450 plus), red free and FA frames (Canon 60 fundus camera; Topcon TRC-50 retinal camera; Zeiss FF 450 plus). OCT examination was performed with Stratus OCT 3000 (OCT3, Carl Zeiss Meditec, Inc., Dublin, CA, USA). For each eye, OCT examination included six 6-mm radial scans, centered on the fovea, and central subfield mean thickness (CSMT) was measured automatically using the macular map software with the 3.45-mm diameter display. A minimum of six vertical or horizontal adjunctive scans of 5 mm were performed as well, positioned so that the cross sectional cut would go through the flecks based on color fundus photography and fundus autofluorescence. In addition, as part of this study, we performed fundus-related perimetry using the MP-1 (MP-1 Micro Perimeter, Nidek Technologies, Padova, Italy) in 12 eyes from 6 of these 32 consecutive patients, and in all control eyes (60 eyes).

Statistical calculations were performed using Epinfo 3.3 software package (CDC, Atlanta). The Mann-Whitney/Wilcoxon two-sample test was used to compare foveal thickness in STGD/FFM patients and in matched healthy control subjects, to assess the influence of foveal thinning on BCVA and on fixation location and stability, and to define a possible correlation between retinal flecks and both foveal thinning and BCVA. We also performed linear regression analysis to compare BCVA and macular thickness. The chosen level of statistical significance was $p < 0.05$.

RESULTS

A summary of clinical findings is presented in Tables I and II. A total of 61 eyes (32 patients, 21 men and 11 women, mean age 43.2 years, range 21–71 years, average) were included in this study: both eyes of 29 patients and one eye of 3 patients. One patient (Case 1, RE) presented with a unilateral epiretinal membrane and thus only the left eye was included. Two patients (Case 17, RE and Case 21, LE) presented with choroidal neovascularization and, therefore, only the fellow eye was included. The age ranged from 21 to 72 years (average 45.8 years) in control subjects (18 men, 12 women). BCVA ranged from 20/20 to 20/400 and from 20/20 to 20/32, respectively, in STGD/FFM patients and in controls.

Color fundus photography revealed in all STGD/FFM patients a various grade of atrophic changes within the macular area as well as the retinal flecks which, in heterogeneous patterns, were perifoveolar or widely distributed in the fundus. These retinal flecks were more prominently visible in the red free frames in comparison with the color photographs. Autofluorescent frames clearly delineated,

TABLE I - PATIENT DATA

Patient	Sex	Age, yr	Eye	Visual acuity–fixation	Mean macular thickness (µm)	Flecks type 1/total scans	Flecks type 2/total scans
1	M	58	RE	20/50	323	Not included	Not included
			LE	20/40	166	4/12	3/12
2	F	23	RE	20/125	139	7/12	6/12
			LE	20/160	152	3/12	0/12
3	M	33	RE	20/50	186	3/6	1/6
			LE	20/20	169	1/6	2/6
4	M	41	RE	20/32	181	3/12	0/12
			LE	20/50	151	1/12	2/12
5	F	23	RE	20/125	132	6/12	3/12
			LE	20/160	151	5/12	2/12
6	M	59	RE	20/25	215	2/6	0/6
			LE	20/40	184	3/6	4/6
7	M	26	RE	20/160	161	5/12	3/12
			LE	20/160	142	5/12	3/12
8	M	26	RE	20/320	121	2/6	6/6
			LE	20/250	123	2/6	4/6
9	F	41	RE	20/80	105	5/12	4/12
			LE	20/63	128	4/12	4/12
10	M	47	RE	20/40	97	3/12	1/12
			LE	20/50	118	2/12	1/12
11	M	66	RE	20/25	206	4/6	6/6
			LE	20/32	220	1/6	3/6
12	F	44	RE	20/40	124	4/6	2/6
			LE	20/20	126	1/6	3/6
13	F	33	RE	20/80	168	5/10	1/10
			LE	20/63	153	5/12	5/12
14	M	38	RE	20/63	147	3/6	0/6
			LE	20/200	141	3/6	3/6
15	M	51	RE	20/40	180	6/6	6/6
			LE	20/32	178	6/6	6/6
16	M	71	RE	20/40	190	5/7	6/7
			LE	20/160	154	10/12	9/12
17	M	58	RE	20/200	210	5/7	5/7
			LE	20/40	133	10/12	9/12
18	F	24	RE	20/200	161	7/12	10/12
			LE	20/200	194	5/12	7/12
19	F	55	RE	20/20	212	2/12	4/12
			LE	20/400	238	0/12	6/12
20	F	41	RE	20/32	190	3/6	1/6
			LE	20/32	180	2/6	1/6
21	F	70	RE	20/25	197	4/6	3/6
			LE	20/200	374	Not included	Not included
22	M	26	RE	20/50	163	2/10	0/10
			LE	20/63	157	5/10	2/10
23	M	45	RE	20/25	178	8/10	7/10
			LE	20/25	181	7/10	6/10
24	M	32	RE	20/63	144	3/6	2/6
			LE	20/25	164	0/12	1/12
25	M	58	RE	20/400	101	0/12	1/12
			LE	20/63	131	2/12	0/12
26	M	29	RE	20/100	132	5/6	2/6
			LE	20/63	136	5/6	0/6
27	F	63	RE	20/50; Stable eccentric	188	2/12	3/12
			LE	20/40; Stable eccentric	172	6/12	4/12
28	M	21	RE	20/125; Unstable eccentric	132	3/6	2/6
			LE	20/160; Unstable eccentric	121	2/6	0/6
29	F	48	RE	20/50; Stable eccentric	155	2/6	2/6
			LE	20/20; Stable central	165	4/6	2/6
30	M	33	RE	20/32; stable central	172	2/12	0/12
			LE	20/50; Stable eccentric	185	2/12	2/12
31	M	56	RE	20/125; Unstable eccentric	159	3/12	2/12
			LE	20/160; Unstable eccentric	114	6/12	4/12
32	M	43	RE	20/25; Stable central	182	2/12	0/12
			LE	20/40; Stable central	157	4/12	6/12

TABLE II - CONTROL DATA

Subject	Sex	Age, yr	Eye	Visual acuity–fixation	Mean macular thickness (μm)
1	M	31	RE	20/20; Stable central	238
			LE	20/20; Stable central	210
2	F	26	RE	20/20; Stable central	214
			LE	20/20; Stable central	214
3	M	36	RE	20/20; Stable central	226
			LE	20/20; Stable central	253
4	M	49	RE	20/20; Stable central	196
			LE	20/20; stable central	211
5	F	23	RE	20/20; Stable central	210
			LE	20/20; Stable central	205
6	M	59	RE	20/20; Stable central	212
			LE	20/32; Stable central	193
7	M	28	RE	20/20; Stable central	218
			LE	20/20; Stable central	216
8	M	26	RE	20/20; Stable central	235
			LE	20/20; Stable central	218
9	F	41	RE	20/25; Stable central	182
			LE	20/20; Stable central	188
10	M	65	RE	20/32; Stable central	172
			LE	20/25; Stable central	196
11	M	28	RE	20/20; Stable central	246
			LE	20/20; Stable central	237
12	F	57	RE	20/25; Stable central	185
			LE	20/20; Stable central	196
13	M	39	RE	20/20; Stable central	214
			LE	20/20; Stable central	202
14	M	55	RE	20/25; Stable central	193
			LE	20/20; Stable central	210
15	F	55	RE	20/25; Stable central	250
			LE	20/32; Stable central	178
16	M	71	RE	20/32; Stable central	250
			LE	20/20; Stable central	229
17	F	21	RE	20/20; Stable central	236
			LE	20/20; Stable central	237
18	M	36	RE	20/20; Stable central	195
			LE	20/20; Stable central	186
19	M	72	RE	20/20; Stable central	205
			LE	20/20; Stable central	203
20	F	54	RE	20/20; Stable central	210
			LE	20/25; Stable central	190
21	F	65	RE	20/20; Stable central	232
			LE	20/20; Stable central	194
22	F	30	RE	20/25; Stable central	167
			LE	20/20; Stable central	186
23	M	47	RE	20/20; Stable central	233
			LE	20/20; Stable central	219
24	M	49	RE	20/20; Stable central	196
			LE	20/20; Stable central	211
25	M	66	RE	20/20; Stable central	226
			LE	20/20; Stable central	204
26	M	46	RE	20/20; Stable central	211
			LE	20/20; Stable central	200
27	F	45	RE	20/20; Stable central	227
			LE	20/20; Stable central	218
28	M	40	RE	20/20; Stable central	188
			LE	20/20; Stable central	188
29	F	53	RE	20/25; Stable central	249
			LE	20/25; Stable central	248
30	F	61	RE	20/20; Stable central	192
			LE	20/20; Stable central	206

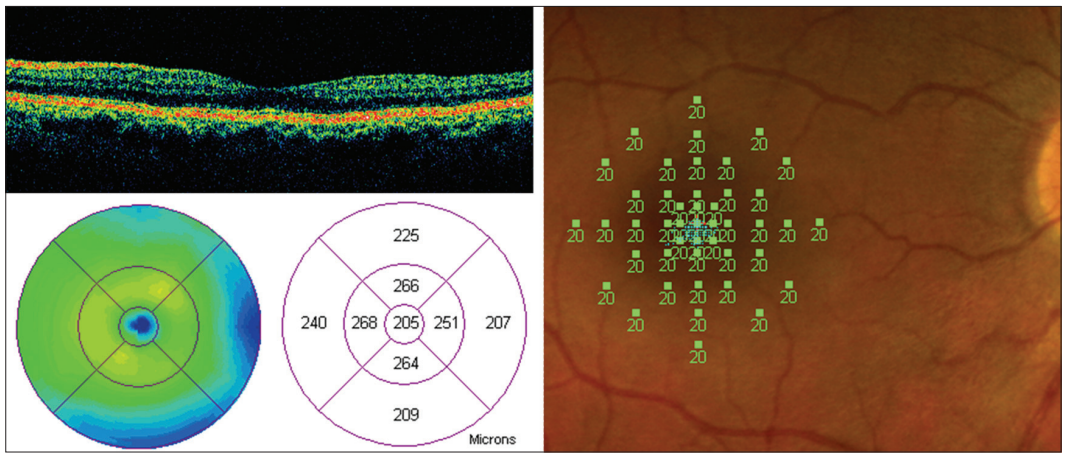

Fig. 1 - *Optical coherence tomography (OCT) scan of a 23-year-old healthy individual (Control 5, LE) with no pathologic signs in the retina or in the retinal pigment epithelium (top left panel). Foveal thickness measured automatically using the macular map OCT-3 software was 205 µm (bottom left panel). Fundus-related perimetry revealed a stable and predominantly central fixation (right panel).*

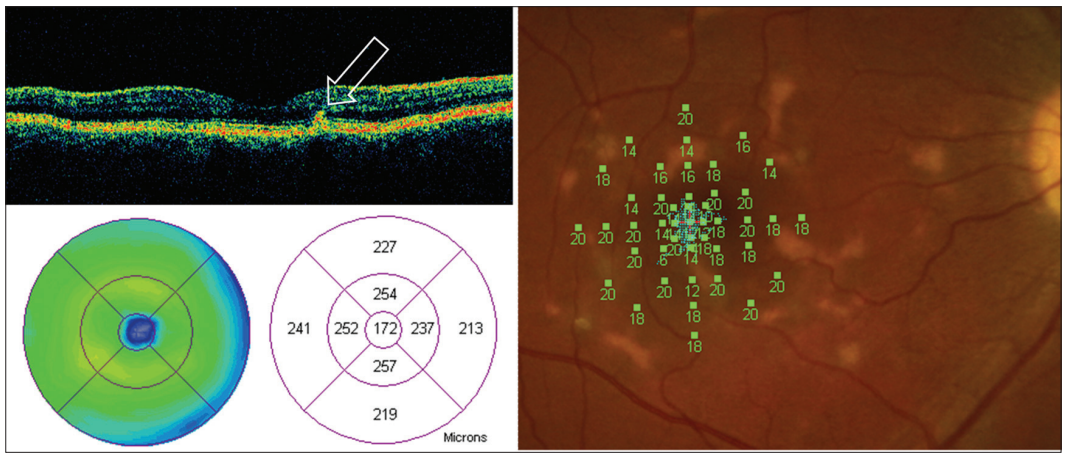

Fig. 2 - *Optical coherence tomography (OCT) scan of a 33-year-old male patient (Patient 30, RE) showing almost normal retinal layers (top left panel) with presence of a type 1 fleck (open arrow). Foveal thickness measured automatically using the macular map OCT-3 software was 172 µm (bottom left panel). Fundus-related perimetry revealed a stable and predominantly central fixation (right panel).*

in all eyes, the retinal flecks as well as areas of profound retinal atrophy. On FA, the retinal flecks appeared as ill-defined areas of hypofluorescence, surrounded by halos of hyperfluorescence corresponding to changes in the RPE. In accordance with the strict criteria for inclusion, dark choroid was present in all the study eyes.

Patients with STGD/FFM presented with a markedly thinned retina in the foveola (mean foveal thickness ranged between 97 and 238 µm, average 160 µm) compared with healthy control subjects (mean foveal thickness ranged between 167 and 253 µm, average 210 µm; $p<0.001$), as evaluated by OCT Stratus. This finding seems to represent a marker of the possible evolution towards foveal atrophy and probably explains the progressive visual loss.

In fact, in our series, comparing mean BCVA with macular thickness, BCVA impairment showed a strong statistically significant correlation to the degree of foveal thinning ($p=0.0029$) ($r^2=0.16$; $p=0.0014$). Moreover, in FFM/STGD patients we observed hyperreflective deposits which we classified into two types: type 1 lesions (29/32 eyes) presented as dome-shaped deposits located in the inner part of the retinal pigment epithelium (RPE) layer and type 2 lesions (22/32 eyes) presented as small linear deposits located at the level of the outer nuclear layer and clearly separated from the RPE layer. Neither of the two types of hyperreflective lesions was correlated with a specific phenotype of the flecks. Based on these findings, we compared mean BCVA with the number of type 1 lesions/total OCT scans subdivided into two groups (< or > median value, each group respectively) ($p=0.2379$) and mean BCVA with the number of type 2 lesions/total OCT scans subdivided, again, into two groups (< or > median value, each group respectively) ($p=0.7653$); further, we compared the mean number of type 1 lesions/total OCT scans with BCVA ($p=0.5700$) and the mean number of type 2 lesions/total OCT scans with BCVA ($p=0.1257$). Moreover, we compared the mean foveal thickness with the number

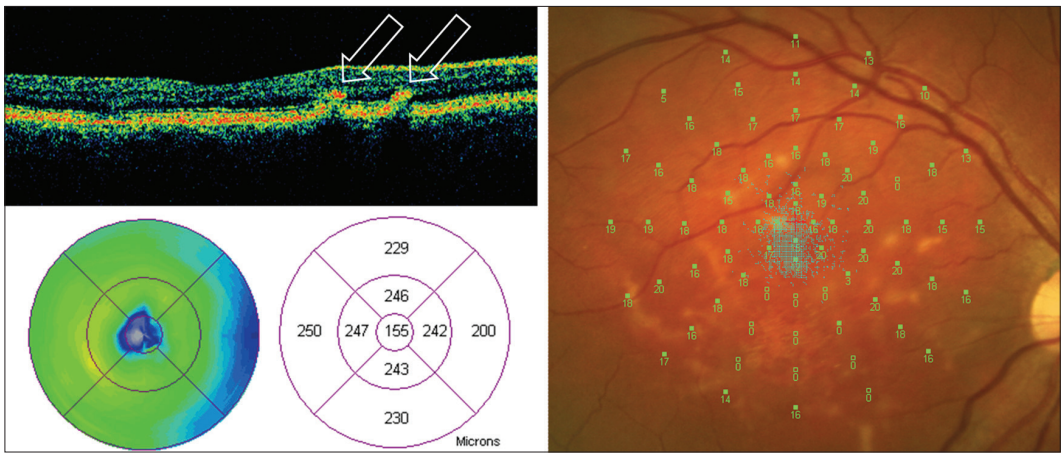

Fig. 3 - *Optical coherence tomography (OCT) scan of a 48-year-old female patient (Patient 29, RE) showing some irregularities of retinal layers in macular area (top left panel) with presence of type 2 retinal flecks (open arrows). Foveal thickness measured automatically using the macular map OCT-3 software was 155 µm (bottom left panel). Fundus-related perimetry revealed a stable and eccentric fixation, located on the border of the scotomata (right panel).*

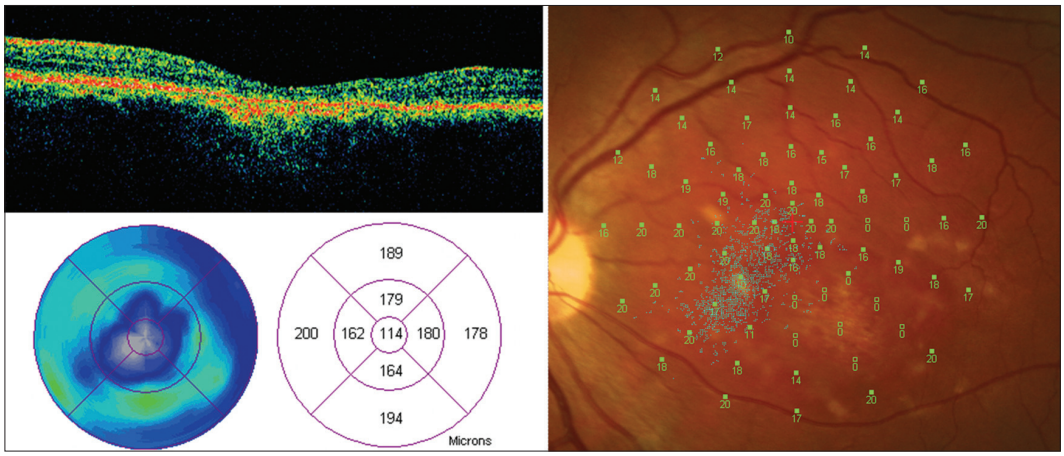

Fig. 4 - *Optical coherence tomography (OCT) scan of a 56-year-old male patient (Patient 31, LE) showing some irregularities and atrophic aspects of retinal layers in macular area (top left panel). Foveal thickness measured automatically using the macular map OCT-3 software was 114 µm (bottom left panel). Fundus-related perimetry revealed an unstable and eccentric fixation (right panel).*

of type 1 lesions/total OCT scans subdivided into two groups (< or > median value, each group respectively) (p=0.8819) and with the number of type 2 lesions/total OCT scans subdivided into two groups (< or > median value, each group respectively) (p=0.6255). Following the statistical analysis, neither of the two types of hyperreflective lesions was correlated with either BCVA impairment or foveal thinning.

In addition, fundus-related perimetry, which was performed in 12 of the study eyes (6 patients), revealed a stable fixation in 8 eyes that was predominantly central (located on the border of the scotomata) in only 4 of these eyes. A more stable fixation (p=0.0108), even if not predominantly central (p value=0.0218), correlated well to a lesser degree of foveal thinning. In all control eyes (60 eyes), fundus-related perimetry revealed a stable and predominantly central fixation.

The OCT macular scan of a 23-year-old healthy individual (Control 5, LE) with no pathologic signs in the retina or in the retinal pigment epithelium is shown in Figure 1. BCVA was 20/20, foveal thickness was 205 µm, and fundus-related perimetry revealed a stable and predominantly central fixation. For comparison, Figure 2 shows the macular scan of a 33-year-old male patient (Patient 30, RE). His BCVA was 20/32 in the presented eye, with a foveal thickness of 172 µm. Fundus-related perimetry revealed a stable and predominantly central fixation. Figure 3 shows the macular scan of a 48-year-old female patient (Patient 29, RE). Her BCVA was 20/50 in the presented eye, with a foveal thickness of 155 µm. Fundus-related perimetry revealed a stable and eccentric fixation, located on the border of the scotomata. Figure 4 shows the macular scan of a 56-year-old male patient (Patient 31, LE). His BCVA was 20/160 in the presented eye, with a foveal thickness of 114 µm. Fundus-related perimetry revealed an unstable and eccentric fixation.

DISCUSSION

To date we have several morphologic and functional tools for evaluation and diagnosis of STGD and FFM. Autofluorescence of the flecks represents one effective method (19-21). FA examination shows early hypofluorescence corresponding to the area of whitish material and central staining of variable intensity without leakage in the late phase; sometimes the hypofluorescence persists until the late phase without staining. Moreover, FA reveals the characteristic phenomenon of dark choroid and displays the entity of macular atrophy. ICG shows the hypofluorescence of the flecks that persists until the late phase with the apparition of the characteristically hyperfluorescent pinpoints (16).

OCT is a noninvasive technique based on low interferometry that provides optical cross-sectional images of the retina and morphologic information close to that obtained from histologic sections. In STGD/FFM patients, as reported by Ergun et al (17) using UHR-OCT, OCT reveals irregularities or defect at the level of photoreceptors layers in macular area. At advanced stages of the disease a profound atrophy of all retinal layers can be observed at the posterior pole, and, as reported by Hargitai et al (18), even a significant correlation between visual acuity and total macular volume and between visual acuity and foveolar thickness, as evaluated by OCT.

We compared BCVA with foveal thickness, a morphologic measure of the retina evaluated by OCT-3, in a consecutive series of 32 patients with STGD/FFM. According to our results, BCVA and foveal thickness were decreased in patients compared with healthy individuals. Following the statistical analysis, we found a linear correlation between BCVA and foveal thickness. Thus, foveolar thinning seems to reflect the degeneration of the foveal photoreceptors, where the density of cones is the highest in the retina, and explains the loss of detailed vision.

Furthermore, in these patients, we compared the type of retinal flecks (little deposits at the level or above the RPE layer, respectively type 1 and type 2) (16), a morphologic feature of the retina evaluated by OCT-3, with BCVA and foveal thickness. The statistical analysis showed that neither of the two types of hyperreflective lesions was correlated with either BCVA impairment or foveal thinning.

Despite several lines of evidence suggesting that the two types of retinal flecks merely reflect different stages of the same disorder, as already reported in a previous study by us (16) (the two types observed simultaneously in 80% of the study eyes; the two types in both eyes of all patients; intermediate aspect, sharing common features between types 1 and 2), one could speculate that the lack of correlation with BCVA and foveal thinning would be possibly due to a still intact photoreceptor layer close to a more or less thin foveola. In fact, one could imagine that an intact photoreceptor layer, not necessarily related to the degree of foveal thinning, as reported by Ergun et al (17), would be a strong bias that does not allow defining a definitive pattern of flecks in relation to the disease progression. This feature could give the reason for a discrepancy between the anatomic fovea centralis and the fixating fovea, especially in case of moderate atrophy, and this, performing OCT scans, should always be considered.

Supporting this hypothesis is the fact that, in our patients, fundus-related perimetry revealed a fixation that was stable, but located eccentrically, even in case of central atrophy. In fact, as the destructive process involves more and more of the fovea, the point of fixation shifts towards the less thin (intact photoreceptor layer) foveal periphery (new preferred retinal locus [PRL]), where the retinal structure still supports detailed vision. Thus, a PRL would be a further bias, again not related to the degree of foveal thinning, in the definition of definitive pattern of flecks in relation to the disease progression. On the other hand, the profound atrophy of all retinal layers at the posterior pole at advanced stages of the disease, a morphologic measure stronger than any bias, explains the statistically significant correlation between foveal thinning and BCVA impairment and unstable fixation, in our and other series (17, 18).

Our study has several limitations. First, although the sample size in the present study is one of the largest in the literature, it was still relatively small, and this might have limited our power in detecting other less important predictors; moreover, our series of patients is even smaller if we look at only the 12 eyes in which fundus-related perimetry was performed. However, patient numbers were large enough to measure a statistical difference. Second, we compared mean BCVA and mean foveal thickness with the number of type 1 and type 2 lesions/total OCT scans, and not with the total number of fundus lesions as visualized by OCT, because not all flecks were scanned by OCT. Third, OCT examination (six 6-mm radial scans) and CSMT were centered on the fixating fovea, which, in such patients, does not correspond necessarily to the fovea centralis; moreover, given that in these patients inability to fixate causes motion artifacts in the OCT im-

ages, computer correction for axial eye motion could have eliminated the ability to visualize true retinal topography.

In conclusion, given that there are few contributively anatomopathologic studies, except the one by Klein and Krill (22) and the one by Eagle et al (23), OCT is a noninvasive useful instrument that provides new information comparable to conventional histopathology (24-26) to better define STGD/FFM. OCT-3 allows an in vivo visualization and quantification of transverse retinal loss, and allows us to define a correlation between foveal thickness and visual function as well as to follow the disease progression in anatomic and functional terms. Fundus-related perimetry is a useful new tool that allows us to better define the degree of functional impairment as well as to demonstrate a more favorable form of the disease in case of development of a PRL.

The authors have no proprietary interest in the materials used in this study.

Reprint requests to:
Giuseppe Querques, MD
Policlinico Riuniti di Foggia
University of Foggia
Viale Pinto, 1
71100 Foggia, Italy
giuseppe.querques@hotmail.it

REFERENCES

1. Stargardt K. Ueber familiare progressive degeneration in der makulagegend des Auges. Albrecht V Graefes Arch Ophthalmol 1909; 71: 534-50.
2. Cibis GW, Morey M, Karris DJ. Dominantly inherited macular dystrophy with flecks (Stargardt). Arch Ophthalmol 1980; 98: 1785.
3. Merlin S, Landau J. Abnormal findings in relatives of patients with juvenile hereditary macular degeneration (Stargardt's disease). Ophthalmologica 1970; 161: 1.
4. Franceschetti A, Francois J. Fundus flavimaculatus. Arch Ophthalmol Rev Gen Ophthalmol 1965; 25: 505-30.
5. Allikmets R, Singh N, Sun H, et al. A photoreceptor cell-specific ATP-binding transporter gene (ABCR) is mutated in recessive Stargardt macular dystrophy. Nat Genet 1997; 15: 236-46.
6. Cremers FP, van de Pol DJ, van Driel M, et al. Autosomal recessive retinitis pigmentosa and cone-rod dystrophy caused by splice site mutations in the Stargardt's disease gene ABCR. Hum Mol Genet 1998; 7: 355-62.
7. Rozet JM, Gerber S, Souied E, et al. Spectrum of ABCR gene mutations in autosomal recessive macular dystrophies. Eur J Hum Genet 1998; 6: 291-5.
8. Aaberg TM. Stargardt's disease and fundus flavimaculatus: evaluation of morphologic progression and intrafamilial co-existence. Trans Am Ophthalmol Soc 1986; 84: 453-87.
9. Lois N, Holder GE, Bunce C, Fitzke FW, Bird AC. Phenotypic subtypes of Stargardt macular dystrophy-fundus flavimaculatus. Arch Ophthalmol. 2001; 119: 359-69.
10. Rotenstreich Y, Fishman GA, Anderson RJ. Visual acuity loss and clinical observations in a large series of patients with Stargardt disease. Ophthalmology 2003; 110: 1151-8.
11. Gerth C, Andrassi-Darida M, Bock M, Preising MN, Weber BH, Lorenz B. Phenotypes of 16 Stargardt macular dystrophy/fundus flavimaculatus patients with known ABCA4 mutations and evaluation of genotype-phenotype correlation. Graefes Arch Clin Exp Ophthalmol 2002; 240: 628-38.
12. Klevering BJ, van Driel M, van de Pol DJ, Pinckers AJ, Cremers FP, Hoyng CB. Phenotypic variations in a family with retinal dystrophy as result of different mutations in the ABCR gene. Br J Ophthalmol 1999; 83: 914-8.
13. Holz FG. Autofluorescence imaging of the macula. Ophthalmologe 2001; 98: 10-8.
14. Von Ruckmann A, Fitzke FW, Bird AC. In vivo autofluorescence in macular dystrophies. Arch Ophthalmol 1997; 115: 609-15.
15. Souied E, Kaplan J, Coscas G, et al. Macular dystrophies. J Fr Ophtalmol 2003; 26: 743-62.
16. Querques G, Leveziel N, Benhamou N, Voigt M, Soubrane G, Souied EH. Analysis of retinal flecks in fundus flavimaculatus using optical coherence tomography. Br J Ophthalmol 2006; 90: 1157-62.
17. Ergun E, Hermann B, Wirtitsch M. Assessment of central visual function in Stargardt's disease/fundus flavimaculatus with ultrahigh-resolution optical coherence tomography. Invest Ophthalmol Vis Sci 2005; 46: 310-6.

18. Hargitai J, Zernant J, Somfai GM, et al. Correlation of clinical and genetic findings in Hungarian patients with Stargardt disease. Invest Ophthalmol Vis Sci 2005; 46: 4402-8.
19. Holz FG. Autofluorescence imaging of the macula. Ophthalmologe 2001; 98: 10-8.
20. Von Ruckmann A, Fitzke FW, Bird AC. In vivo autofluorescence in macular dystrophies. Arch Ophthalmol 1997; 115: 609-15.
21. Bellmann C, Hvlz FG, Schapp O, et al. Topography of fundus autofluorescence with a new confocal scanning laser ophthalmoscope. Ophthalmologe 1997; 94: 385-91.
22. Klein BA, Krill AE. Fundus flavimaculatus. Clinical, functional and histopathological observations. Am J Ophthalmol 1967; 64: 3-23.
23. Eagle RC, Lucier AC, Bernadrdino VB, Yanoff M. Retinal pigment abnormalities in fundus flavimaculatus. Ophthalmology 1980; 87: 1189-200.
24. Gloesmann AM, Hermann B, Schubert C, Sattmann H, Ahnelt PK, Drexler W. Histological correlation of pig retinal stratification with ultrahigh resolution optical coherence tomography. Invest Ophthalmol Vis Sci 2003; 44: 1696-703.
25. Drexler W, Morgner U, Ghanta RK, et al. ultrahigh resolution ophthalmologic optical coherence tomography. Nat Med 2001; 7: 502-7.
26. Anger EM, Unterhuber A, Hermann B, et al. Ultrahigh resolution optical coherence tomography of the monkey fovea: identification of retinal sublayers by correlation with semi-thin histology sections. Exp Eye Res 2004; 78: 1117-25.